JOURNAL OF MATERIALS SCIENCE 25 (1990) 2465–2470

Crystallization of acicular platelet particles of W-type hexagonal strontium ferrite for magnetic recording applications

SHANKER RAM*
Department of Materials Science and Engineering, McMaster University, Hamilton, Ontario L8S 4L7, Canada

Acicular platelets of the W-type hexagonal strontium ferrite ($SrFe_{18}O_{27}$) have been crystallized from the borate glass system with the aid of ~1 mol% SiO_2 and Bi_2O_3. It was found that particle size and morphology of the system can be effectively altered by proper use of the additives and the thermal treatment of the samples. Addition of SiO_2 induces growth of ferrite as fine grains (average size ~0.1 μm), while Bi_2O_3 with the acicular-shaped particles (which are platelets) with an aspect ratio of ~10 are formed. The system also exhibits a relatively sharp particle size distribution compared to that for the samples containing no additive. Detailed magnetic and microstructural measurements of all the useful samples were carried out to characterize them for applications in magnetic recording devices.

1. Introduction

The recent advances of hexagonal ferrites in magnetic recording heads, microwave devices and most other technological applications demand the development of specimens with discrete (and homogeneous) microcrystalline particles grown specifically in acicular-shaped platelets [1–5]. These platelets are easily coated with the plastic or rubber base (while making the particular device) and ensure better reliability than do thin films, and will definitely replace the use of the latter in the near future. The acicular nature of the particles induces a magnetic shape anisotropy, $H_b = 4\pi M_s$ ($H_b = \frac{1}{3}\pi M_s$ for spherical particles), which helps alignment of the particles in the direction of the crystalline axis by the applied magnetic field [4], where M_s is the saturation magnetization.

During the last decade, several investigations including material processings have been carried out to fabricate the acicular platelets of ferrites [4–8]. The crystallization of hexagonal ferrites (M- and W- type) based on calcium and barium compositions in a borate glass matrix have been reported [8–10]. From the viewpoint of particle shape and dispersibility, this process has been found to be one of the most superior methods for production of the ferrites. However, using the ordinary glass crystallization method, it was found difficult to produce platelet particles with good reproducibility whose average size was less than 1 μm. The particle distribution was often not very sharp. Therefore, in order to improve the particle size characteristics we continued the experiments using several additives, such as Ag_2O, SiO_2, Bi_2O_3, P_2O_5, etc.

The present article reports the results obtained on W-type hexagonal strontium ferrite precipitated in the $SrO–Fe_2O_3–B_2O_3$ system with the aid of 1 mol% SiO_2 and Bi_2O_3. The influence of the additives on microstructure and intrinsic magnetic properties of the material are discussed.

2. Experimental details

The compositions of the glasses studied in this work are given in Table I. Glass batches were melted using reagent grade chemicals in alumina crucibles at a temperature ~1650 K. The molten glass was poured between rotating twin rolls [9], and quenched into flakes at 77 K by using liquid nitrogen as a coolant. The specimens with all compositions were completely amorphous as confirmed by X-ray diffractometry.

The glass transition (T_g) and crystallization temperatures were estimated from differential thermal analysis (DTA) [8]. The specimens then were heat-treated in order to induce crystallization (cf. results in Table II). The particle size and morphology of the resulting crystallites were analysed using a Zeiss optical microscope, a Phillips TEM-301 electron microscope and a Bausch and Lomb image analyser (model 500).

Magnetization measurements of the various samples were made using a Varian V-7200 magnet in conju-

TABLE I Summary of the glass compositions

Series	Constituents (mol %)				
	SrO	Fe_2O_3	B_2O_3	SiO_2	Bi_2O_3
A	35	25	40	–	–
B	40	25	35	–	–
C	47	25	28	–	–
D	47	25	27	1	–
E	47	25	27	–	1
F	47	25	26	1	1

*Visiting Scientist.

0022–2461/90 $03.00 + .12

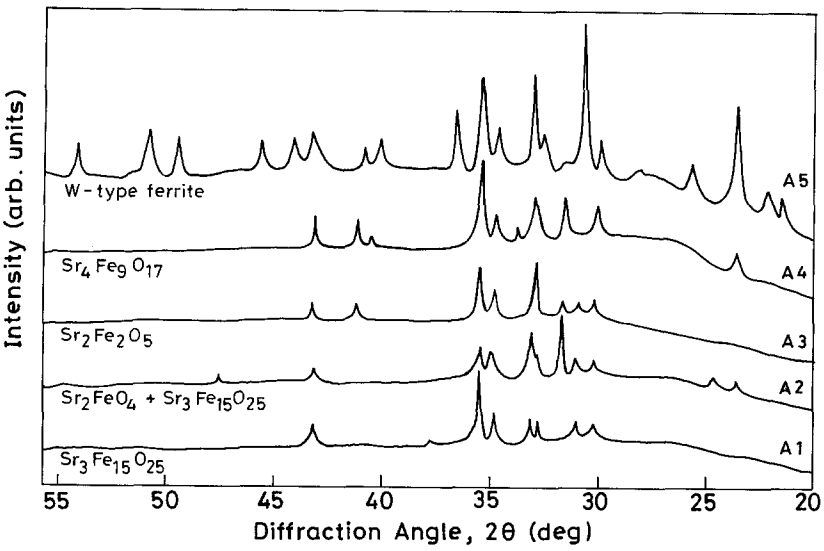

Figure 1 X-ray diffraction patterns showing crystallization of different crystallite phases in glass composition series A.

gation with a PAR Vibrating Sample Magnetometer (model 150A). A high-temperature oven assembly (model 151) coupled with the magnetometer was employed for the temperature-dependence studies of the magnetization. A homemade dewar containing liquid nitrogen as the coolant was used for measurements below room temperature.

3. Results and discussion

3.1. Crystallization of ferrite particles

The typical glass composition series given in Table I show completely amorphous behaviour. Their X-ray diffractograms also do not reveal any diffraction line characteristic of a crystalline phase. The samples readily crystallize out with ferrite magnetic phases when subjected to thermal treatments. The results of crystallization, magnetic properties and the heat-treatment schedule of the samples are summarized in Table II.

Formation of the crystalline phases in the SrO–Fe_2O_3–B_2O_3 glass system appears to be a strong function of the glass composition (Table I) used in the initial and heat-treatment schedule. The various crystalline phases found to precipitate in the system were (i) γ-Fe_2O_3, (ii) α-Fe_2O_3, (iii) $Sr_2Fe_2O_5$, (iv) Sr_2FeO_4 and (v) hexagonal strontium ferrites. The typical X-ray diffractograms shown in Fig. 1 clearly demonstrate the crystallization of these phases in different samples of composition series A. The W-type ($SrFe^{2+}_2Fe^{3+}_{16}O_{27}$) hexagonal ferrite is precipitated as the only

TABLE II Crystallization, microstructure and magnetic properties of W-type ($SrFe_{18}O_{27}$) ferrite in the various glass systems

Series	Heat-treatment	Crystallites	Magnetization, M_s (e.m.u. g^{-1})	Coercivity, H_c(Oe)	T_c(K)
A1	410 K/5 h 510 K/12 h	$Sr_3Fe_{15}O_{25}$ γ-Fe_2O_3	7.5	310	840
A2	590 K/5 h 630 K/12 h	Sr_2FeO_4 $Sr_3Fe_{15}O_{25}$	6.0	295	840
A3	725 K/2 h 810 K/12 h	$Sr_2Fe_2O_5$	5.0	415	525,825
A4	885 K/5 h 935 K/12 h	$Sr_4Fe_9O_{17}$	6.7	305	450,840
A5	885 K/5 h 1120 K/12 h	W-phase	7.5	385	850
A6	1100 K/2 h 1120 K/20 h	α-Fe_2O_3	2.1	2450	630
B5	885 K/5 h 1120 K/12 h	W-phase α-Fe_2O_3	8.5	400	850
C5	900 K/2 h 1135 K/20 h	W-phase α-Fe_2O_3	9.5	4300	830
C6	1100 K/2 h 1135 K/20 h	$SrFe_{12}O_{19}$	5.4	3200	650
D5	900 K/2 h 1130 K/20 h	W-phase	17.0	4200	820
E5	900 K/2 h 1130 K/20 h	W-phase	25.0	2500	820
F5	900K/2 h 1130 K/20 h	W-phase	30.8	4100	810

crystalline phase in sample A5. $Fe^{3+} \rightleftharpoons Fe^{2+}$ reduction reaction usually takes place in the system and making the ferrite crystal lattice thermally unstable [11]. A $Sr_3Fe_{15}O_{25}$ ferrite (hexagonal crystal structure) phase observed in samples A1 and A2 eventually forms the Sr^{2+}-stabilized W-type ferrite as follows

$$SrFe_2^{2+}Fe_{16}^{3+}O_{27} + 2SrO$$
(W-phase)

$$\underset{\text{reduction}}{\overset{Fe^{3+} \rightarrow Fe^{2+}}{\rightleftharpoons}} Sr_3Fe^{2+}\square Fe_{14}^{3+}O_{25} + FeO$$

where $\square$ denotes an Fe^{2+} vacancy. Likewise, $Sr_4Fe_9O_{17}$ crystallizing out in sample A4 is another Sr^{2+} stabilized M-type ($SrFe_{12}O_{19}$) ferrite. The content of SrO (Table I) in the glass composition series imparts an important role in thermal stability of these ferrites. As a consequence, an increase in SrO to more than 35 mol % in composition series B and C appears to limit the $Fe^{3+} \rightleftharpoons Fe^{2+}$ reduction, and W-type ferrite occurs as the predominant crystalline phase in most of the heat-treatments. It is now also thermally stable. No formation of oxygen deficient ferrites occurs even after a further annealing of the system to ~ 1500 K for several hours.

It is interesting that the W-type ferrite crystallizes out as the only magnetic phase in composition series C; however, the crystallization yield is still not very satisfactory. A major fraction of the reactants SrO and Fe_2O_3 is not utilized in the ferrite formation reaction. Addition of 1 mol % SiO_2 or Bi_2O_3 to this particular composition series markedly increases the nucleation of W-phase ferrite, thus showing a crystallization yield of ~ 21.5 and 32.0 wt % (estimated using the crystallization volume fraction in microstructure and the bulk density of the system), respectively. The results obtained for the various samples are given in Table III. A surprisingly large yield, i.e. ~ 40 wt %, is found to crystallize out in the system when 1 mol % of both SiO_2 and Bi_2O_3 are used together in sample F5. This is larger by ~ 1.8 wt % than the theoretically calculated yield (cf. Table III), assuming a 100% utilization of the Fe_2O_3 contents in the formation of W-phase ferrite. The discrepancy eventually indicates a participation of some foreign mass, i.e. B_2O_3 or the additives (SiO_2 and Bi_2O_3), in the reaction. These impurities could be incorporated in place of Fe^{3+} vacancies in the ferrite interstitial lattice sites [12, 13]. This is the reason why the relative intensities of the characteristic diffraction lines of ferrite phase [14] vary by a reasonable amount in the case of these samples (for example cf. Fig. 2).

TABLE III Maximum crystallization yields of W-phase ferrite obtained for the various glass-composition systems

Composition series	Crystallization yield (wt %)*		M_s (e.m.u. g^{-1})
	Obs.	Calc.	
A	13.0	41.14	57.7
B	12.0	40.48	70.8
C	12.9	40.33	80.0
D	21.5	40.37	79.1
E	32.0	38.19	78.0
F	40.0	38.22	77.0

*The theoretical yield is estimated for the ferrite phase using the stoichiometric masses of Fe_2O_3 and SrO assuming 100% utilization of the iron oxide in the reaction.

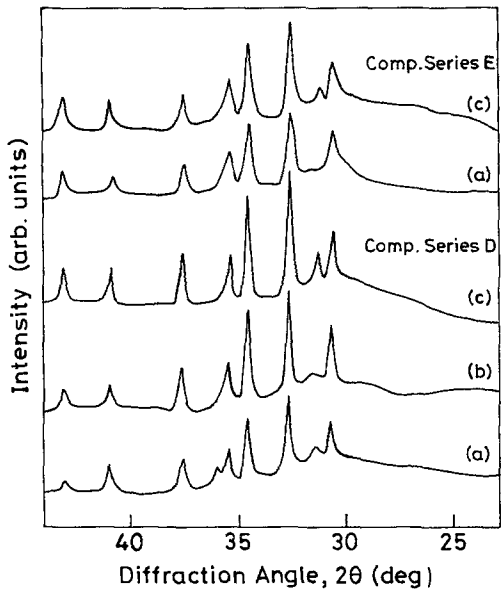

Figure 2 Effect of SiO_2 and Bi_2O_3 additives on the diffraction patterns for W-type ferrite precipitating in composition series D and E, respectively. The samples were heat treated at 900 K/2 h followed by 1130 K for (a) 2, (b) 5 and (c) 20 h.

3.2. Effect of the additives on microstructure of the ferrite systems

The ferrite particles in the present systems are usually crystallized out as acicular platelets. This has been confirmed by microstructure and measurement of the X-ray diffraction patterns of powder and bulk samples. The diffraction patterns reasonably differ in the two cases, i.e. the diffraction lines corresponding to the lattice planes parallel to the c-axis in general exhibit enhanced intensities in the case of the bulk. The features are very similar to those reported for barium or/and calcium ferrites in detail [8–10]. The microstructure indicates the particle size of the samples varies over a wide range, i.e. from a few nanometres to micrometer order. The addition of Bi_2O_3 (1 mol %) to the system favours the growth of ferrite phase with a large aspect ratio of acicular particles. A typical electron micrograph shown in Fig. 3a (samples E5) clearly reveals these platelets (black) of average size $\sim 3\,\mu$m. The corresponding electron diffraction patterns (Fig. 4) exhibit lattice reflections characteristic of single crystals of W-type ferrite. These crystal particles are essentially grown along the c-axis (marked by the arrow in Fig. 3a).

SiO_2 (1 mol %), on the other hand, inhibits grain growth and the acicular shape of the particle. As a result, sample D5 (Fig. 3b) comprises mostly fine particles ($\sim 0.1\,\mu$m size) due to the strontium ferrite. The particle size and particle distribution appear relatively sharper than those obtained without additives or with Bi_2O_3 addition in the sample series C.

More interesting microstructure is observed when the two additives are used together, as in sample F5. As shown in Fig. 5, the particles (white) grow as regular platelets of length $\sim 1\,\mu$m and width $\sim 0.1\,\mu$m.

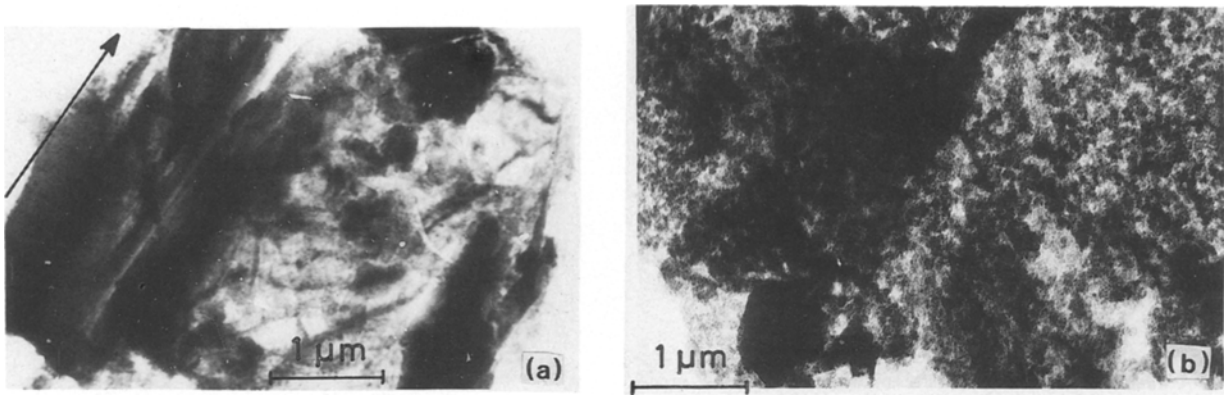

Figure 3 Transmission electron photographs of (a) large acicular platelets (samples E5), and (b) fine particles (sample D5) of W-type ferrite showing the precipitation effect of Bi_2O_3 and SiO_2 additives on the system. The arrow indicates orientation (c-axis) of a typical acicular particle.

The single particle characteristics of the samples are confirmed by analysing the image structure for intercepts. The samples appearing as discrete and isolated particles in the microstructure do not show an intercept; they are the single crystal particles of ferrite. Also, the microstructure studied after etching the surface of the samples with weak acetic acid does not differ significantly. It should be noted that no such fine distribution of ferrite platelets with this large crystallization volume fraction has been reported by any other method [4–6]. The material in this respect appears to be quite suitable for use in perpendicular magnetic recording (it is believed to provide ultra-high recording density [1]). A problem which has yet to be solved is the particle size, which remains larger than the standard size of $\leqslant 0.2\,\mu$m [4].

3.3. Magnetic results

The specific magnetization (M), coercivity (H_c) and remanent magnetization (M_r) for the different samples were studied by measuring the hysteresis loop in the applied magnetic field H. The as-prepared glass samples, as expected, show very low magnetic moments ($\leqslant 0.1$ e.m.u. g^{-1}) and coercive fields $H_c \sim 20$ Oe. The magnetic moment as well as H_c rapidly develops when the specimens are heat-treated as given in Table II. This indicates crystallization of magnetic particles within the glass matrix by the thermal treatments. We are interested in the magnetic properties of these particles.

Fig. 6 shows the magnetization behaviour of typical heat-treated sample measured as a function of H. Most of the samples do not usually show a magnetic saturation. This is often probably due to a small presence of superparamagnetic particles in the system. A wide variation of particle sizes from 0.01 to 5 μm is evident from the microstructure. The particles $\leqslant 0.01\,\mu$m size could impart superparamagnetic behaviour [15]. Absence of the saturation could also have an effect due to co-precipitation of α-Fe_2O_3 phase and/or the presence of Fe cations in different oxidation/co-ordination states [8]. The particle sizes evidently increase and the system shows considerably enhanced crystallization yields and a relatively sharp size distribution of magnetic phase in the samples containing Bi_2O_3/SiO_2 additives. The M–H plots (Fig. 6), in fact, give the magnetic saturation at reasonably smaller magnetic fields, $H \leqslant 20$ kOe, in these particular samples. The value of M_s (the saturation magnetization) for the other samples we have estimated by extrapolating the experimental data following the law of approach to saturation [16]. These values are up to 20% larger than that observed at $H = 20$ kOe. The results for M_s and other magnetic data of coercivity (H_c) and the Curie transition temperature T_c obtained on the useful samples are also included in Table II.

Values of M_s (cf. Tables III) were also estimated for the ferrite particles (excluding the glassy part of the bulk) precipitated in the various composition series. These were obtained simply dividing M_s for the bulk

Figure 4 Electron diffraction patterns of the acicular platelets in Fig. 3a. The electron beam was incident normal to the c-axis.

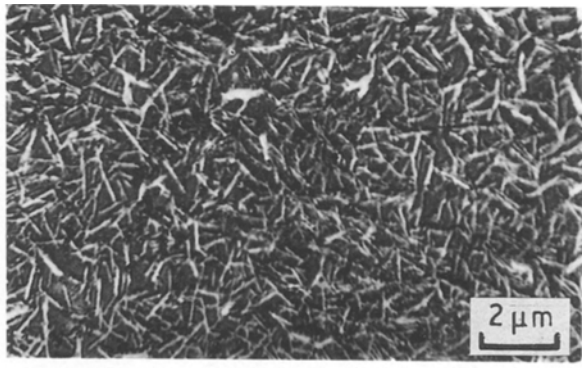

Figure 5 Optical micrograph showing the hexagonal platelets (white) of W-type ferrite precipitated after addition of 1 mol % SiO_2 and Bi_2O_3 in sample F5.

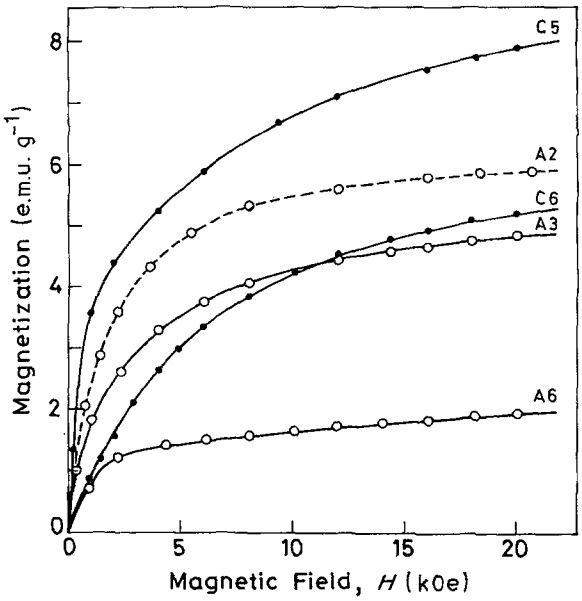

Figure 6 Plot of magnetization, M, as a function of the applied magnetic field, H, for the selected glass-ceramic samples.

specimen by the crystallization yield (given in the same table). The maximum value of $M_s = 80\,\text{e.m.u.g}^{-1}$ thus observed in composition series C is very consistent with that reported for the synthesized W-type ferrite [9, 17]. The other composition series exhibit significantly smaller M_s values, possibly due to the incorporation of some nonmagnetic ions (i.e. B^{3+}, Si^{4+} or Bi^{3+}) impurities as evident by the X-ray diffraction and microstructural analyses. Some incipient growth of iron oxide/M-type ferrite seems responsible for the low estimated M_s values in composition series A and B.

Fig. 7 shows the hysteresis loop obtained for sample F5 which revealed a maximum $M_s = 30.8\,\text{e.m.u.g}^{-1}$ (77 e.m.u.g^{-1} in ferrite particles) for the bulk. This sample also gives rise to a large coercivity, $H_c = 4100$ Oe. The skewness of the M–H loop as measured perpendicular to the platelet samples (cf. Fig. 5) is found to be $M_r/M_s = 0.8$; it is high enough for perpendicular magnetic recording media, and also seems useful for other magnetic device applications [1, 2]. Moreover, the specimens containing Bi_2O_3 additives exhibit feasibly smaller M_r/M_s (~ 0.7) and H_c (~ 2500 Oe) values.

The coercivity is a complicated function of several factors, such as the particle size and morphology, the nonmagnetic impurities incorporated in the interstitial sites, the multidomain nucleation formation, and the strain defects produced in the system during thermal treatments [10, 18–19]. The sample series A and B that do not contain nucleating additives show an order of magnitude lower coercivity ($H_c \leqslant 400$ Oe) compared to sample series C and laters. Such small values of H_c for the W-type ferrite phase are possibly predominant due to the multidomain nucleation formation in the system [18, 19]. In later experiments [19] we have

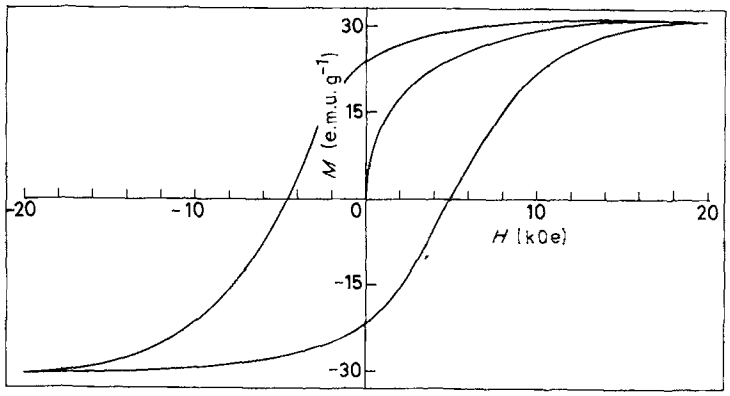

Figure 7 A typical hysteresis loop for the glass-ceramic sample F5.

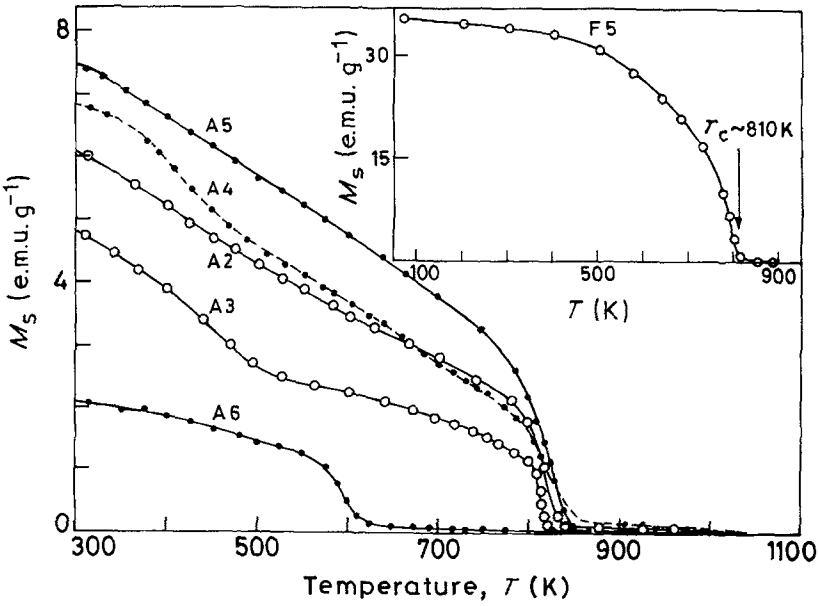

Figure 8 The temperature dependence of the saturation magnetization, M_s. The samples containing SiO_2 or Bi_2O_3 exhibit a relatively steady fall of M_s with temperature, as shown by a representative example of sample F5 in the inset.

observed values of H_c as low as $\leqslant 100$ Oe for similar ferrites synthesized by high-temperature (~ 1650 K) thermal treatments of the stoichiometric composition through ceramic methods. This also demonstrates that the use of Bi_2O_3 and SiO_2 additives in the investigation prevents the multidomain nucleation formation of the ferrite particles.

Examples of our temperature dependence studies of M_s are portrayed in Fig. 8. M_s decreases with increasing temperature and sharply falls to zero at the characteristic Curie transition temperature (T_c) around 830 K for the W-phase ferrite. Sample A6, which does not exhibit X-ray diffraction lines due to the ferrite phase, clearly demonstrates a distinct $T_c \sim 630$ K. Moreover, a marginal variation of T_c (around 830 ± 20 K) also noted for the ferrite phase samples, is in agreement with the nonmagnetic impurities being incorporated into the ferrite particles [17]. Sample F5, which is believed to contain SiO_2 or Bi_2O_3 impurities, reveals a $T_c \sim 810$ K.

Most of the magnetic device applications also require a small magnetization coefficient of temperature ($\partial M_s/\partial T$), at least for the working-temperature range. The ferrite samples which crystallized out with the aid of Bi_2O_3/SiO_2 additives appear quite beneficial in this view. This material series evidently follows a much steadier decrease in M_s ($\partial M_s/\partial T \sim 0.005$ e.m.u. g^{-1} K^{-1} for $T \leqslant 400$ K) as shown for a representative sample, F5, in Fig. 8.

4. Conclusions

Acicular platelets of W-type hexagonal strontium ferrite ($SrFe_{18}O_{27}$), useful especially for magnetic recording applications, were obtained by crystallization in the glass system on addition of 1 mol % SiO_2 and Bi_2O_3. Both additives are found to influence significantly the intrinsic magnetic properties of the material through microstructural developments subjected to the thermal treatments of the specimens. The crystallization yield is also considerably enhanced and the samples show a fairly sharp distribution of particles.

Acknowledgements

The author is grateful to Professor G. P. Johari for a personal discussion and encouragement, and to Professor D. Chakravorty (presently at the Indian Association for the Cultivation of Science, Jadavpur, Calcutta-32, India) for suggesting the problem during my stay at the Indian Institute of Technology, Kanpur-208016, India.

References

1. S. IWASAKI and Y. NAKAMURA, *IEEE Trans. Magn.* **MAG-13** (1977) 1272.
2. O. KUBO, T. IDO and M. YOKOYAMA, *ibid.* **MAG-18** (1982) 112.
3. T. FUJIWARA, *ibid.* **MAG-21** (1985) 1480.
4. Y. OGATA, T. IMURA and H. HARADA, *Adv. Ceram.* **16** (1985) 289.
5. R. ARDIACA, R. RAMOS, A. ISALGUÉ, J. RODRIGÜEZ, X. OBRADORS, M. PERNET and M. VALLET, *IEEE Trans. Magn.* **MAG-23** (1987) 22.
6. M. SUGIMOTO, Y. ARAI and T. NUKUI, *Adv. Ceram.* **16** (1985) 273.
7. F. LICCI and T. BESAGNI, *IEEE Trans. Magn.* **MAG-20** (1984) 1639.
8. S. RAM, D. CHAKRAVORTY and D. BAHADUR, *J. Magn. Magn. Mater.* **62** (1986) 221.
9. S. RAM, D. BAHADUR and D. CHAKRAVORTY, *ibid.* **67** (1987) 378.
10. *Idem, J. Noncryst. Solids* **101** (1988) 227.
11. F. T. LOTGERING and P. H. G. M. VROMANS, *J. Amer. Ceram. Soc.* **60** (1977) 416.
12. F. KOOLS, *Adv. Ceram.* **15** (1985) 177.
13. P. PESHEV and H. PACHEVA, *Mater. Res. Bull* **15** (1980) 1199.
14. A. COLLOMB, P. WOLFERS and X. OBRADORS, *J. Magn. Magn. Mater.* **62** (1986) 57.
15. E. HANGA, E. TATARU, M. MORARIU, L. DIAMANDESCU and N. POPESCU-POGRION, *Phys. Status Solidi (a)* **67** (1981) 725, and references cited therein.
16. R. GRÖSSINGER, *ibid.* **66** (1981) 665.
17. J. P. MIGNOT, P. WOLFERS and J. C. JOUBERT, *J. Magn. Magn. Mater.* **51** (1985) 337.
18. M. VALLET, P. RODRIGÜEZ, X. OBRADORS, A. ISALGUÉ, J. RODRIGÜEZ and M. PERNET, *J. de Phys.* **46** (1985) C6-335.
19. S. RAM, D. BAHADUR and D. CHAKRAVORTY, *J. Magn. Magn. Mater.* **71** (1988) 359.

Received 6 March
and accepted 24 August 1989